Available online at www.sciencedirect.com

SciVerse ScienceDirect

Ceramics International 38 (2012) 4549–4554

CERAMICS INTERNATIONAL

www.elsevier.com/locate/ceramint

# Combustion synthesis of SiC/$Si_3N_4$-NW composite powders: The influence of catalysts and gases

Chao-Sheng Zheng [a], Qing-Zhi Yan [a,*], Min Xia [b]

[a] *Laboratory of Special Ceramics and Powder Metallurgy, University of Science and Technology Beijing, Beijing 100083, People's Republic of China*
[b] *Institute of Powder Metallurgy and Advanced Ceramics, Southwest Jiaotong University, Chengdu 610031, People's Republic of China*

Received 25 September 2011; received in revised form 6 February 2012; accepted 13 February 2012

## Abstract

Composite powders containing silicon carbide (SiC) particles and silicon nitride nanowires ($Si_3N_4$-NWs) were synthesized by combustion synthesis, using elemental Si, carbon black, PTFE and small amount of metal powders as raw materials. The catalyst types and environmental gases and pressures have been altered to study their influence upon the crystal growth and the nature of the products. The products were characterized by X-ray diffraction, scanning and transmission electron microscopy. Results reveal that the metal/silicon liquid (e.g. $Ni_2Si$ and $Fe_3Si$) formed during the combustion process is a key factor for the growth of $Si_3N_4$-NWs in nitrogen. For the process carried out in non-nitrogen gas (Ar, $CO_2$ or mixed $CO_2/O_2$), pure SiC particles were obtained. The rise in nitrogen pressure can promote the growth of $Si_3N_4$-NWs as well as large SiC particles. The growth of $Si_3N_4$-NWs could be explained by the SLGS mechanism, and the growth of SiC particles was involved in the gas-phase and liquid-phase mechanisms.

*Keywords:* D. SiC; D. $Si_3N_4$; Combustion synthesis; Nanowires

## 1. Introduction

Combustion synthesis (CS) is a unique process which involves that the heat generated by an exothermic reaction sustains the reaction itself along a combustion wave after external ignition. CS has attracted especial attention to prepare a large variety of advanced materials such as refractory materials, intermetallic materials, cermets, and superconductors [1,2], since it offers advantages with respect to process economics and process simplicity. SiC and silicon nitride ($Si_3N_4$) based ceramics have been intensively studied over many years for their potential application as structural ceramics at both room and elevated temperatures. For example, SiC based materials have been widely considered as the potential materials for fusion reactors, primarily due to their inherently low induced radioactivities. CS is widely used to fabricate SiC, $Si_3N_4$ and SiC/$Si_3N_4$ composite powders [3–12]. In addition, SiC and $Si_3N_4$ fibers/whiskers have been successfully synthesized by the CS [13–17].

Transition metals, particularly iron, have been widely used as the catalyst for the growth of SiC or $Si_3N_4$ whiskers [18–24], due to their good affinities to the constituent atoms of the whiskers. On the other hand, it is well known that transition metals can regulate kinetics of silicon nitridation as well as α-/β-phase formation [25–31]. Thus transition metals offer an opportunity to regulate SiC/$Si_3N_4$ formation in the Si–C–N system. Recently we reported that [32], for the CS carried out in nitrogen, Fe powders could catalyze in situ formation of $Si_3N_4$-NWs among the SiC particles while pure SiC particles were synthesized for the samples without Fe additives. The as-synthesized SiC/$Si_3N_4$-NW composite powders have great potential in the fabrication of high-performance ceramic composites due to their initially dispersive state.

In the present work, CS was carried out under different parameters (catalyst type, environmental gas and pressure) to optimize the processing parameters, and to study their influence upon the crystal growth and the nature of the products.

## 2. Experimental procedure

Raw materials used in this study included Si powders (1–3 μm, 99% pure), carbon black (24 nm, 99% pure),

---

* Corresponding author. Tel.: +86 010 6233 4951; fax: +86 010 6233 4951.
*E-mail address:* qingzhiyan111@163.com (Q.-Z. Yan).

0272-8842/$36.00 © 2012 Elsevier Ltd and Techna Group S.r.l. All rights reserved.
doi:10.1016/j.ceramint.2012.02.032

polytetrafluoroethylene (PTFE) powders (99% pure) and metal powders (Al, Ti, Ni, or Fe). The starting materials had a mixing ratio of PTFE: (Si + C) = 15:100 (wt), Si:C = 1:1 (mol) and a small amount of metal catalysts. The combustion process was carried out in a high pressure combustion vessel. To optimize the processing parameters and study the influence of parameters upon the crystal growth, the vessel was filled with various gases at different initial pressures, or the experiments were carried out on the samples with different catalyst types. All other variables (e.g. silicon–carbon ratio and PTFE content) were kept constant. The temperature history was recorded by a W-5%Re/W-26%Re thermocouple of Ø0.5 mm, whose tip was embedded in the reactant. After the vessel was cooled down, the gas was vented and the products were collected for further examination. X-ray diffraction (XRD) was used to analyze the solid products. The morphologies were observed by field-emission scanning electron microscope (FESEM). Transmission electron microscope (TEM) was used to further characterize the nanowires.

## 3. Results and discussion

### 3.1. The catalysts

The combustion experiments were initially carried out on the samples with different metal catalysts in nitrogen gas. The morphologies and crystalline structures of the products were analyzed using FESEM (Fig. 1) and XRD (CuKα) (Fig. 2) respectively. In order to clearly exhibit low-intensity peaks (e.g.

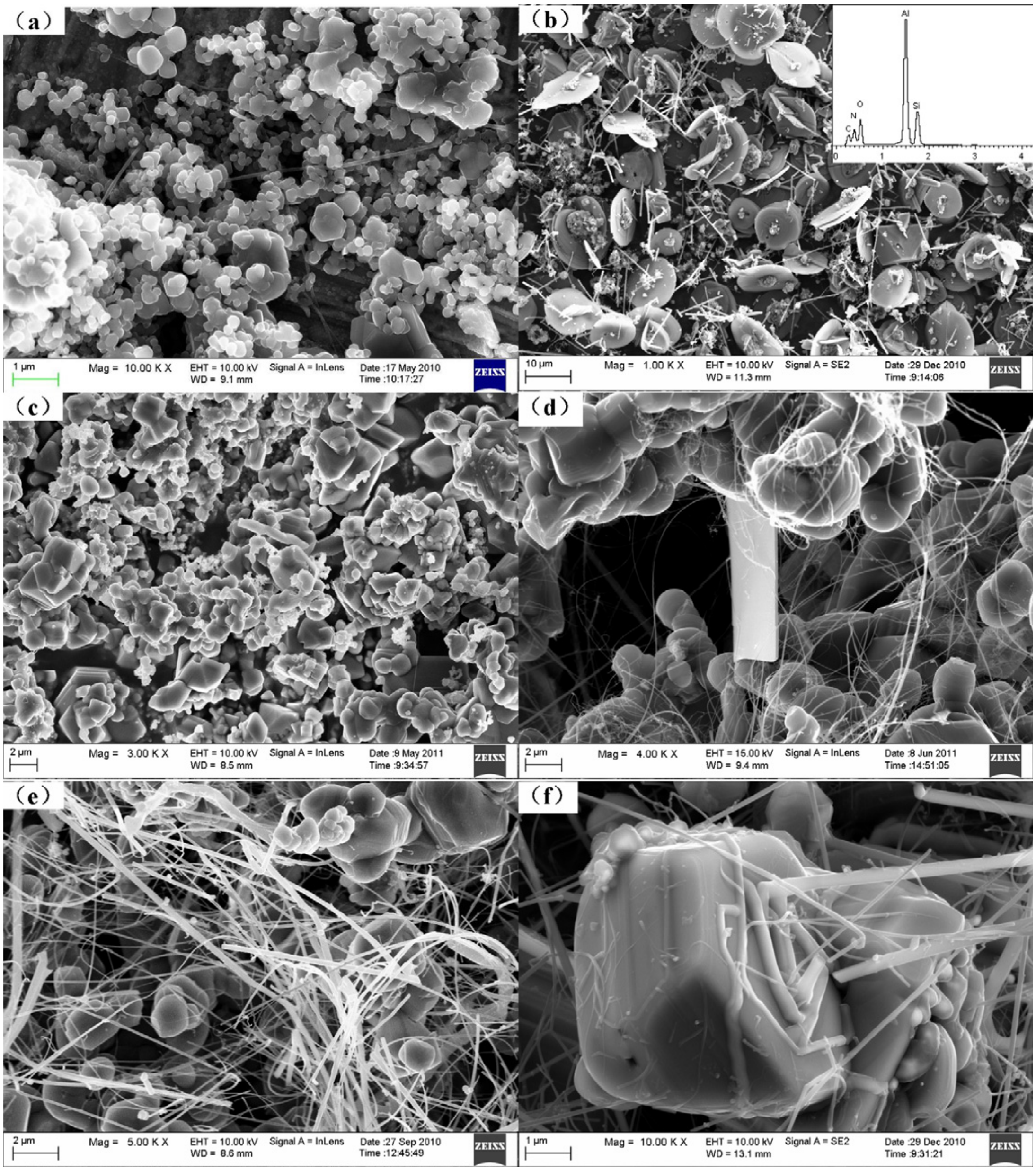

Fig. 1. FESEM images of the products obtained from the samples with different metal catalysts in nitrogen atmosphere: (a) Al; (b) Al, image of white materials from the upper surface with EDS data (inset) of leaf-like crystals; (c) Ti; (d) Ni; (e) and (f) Fe.

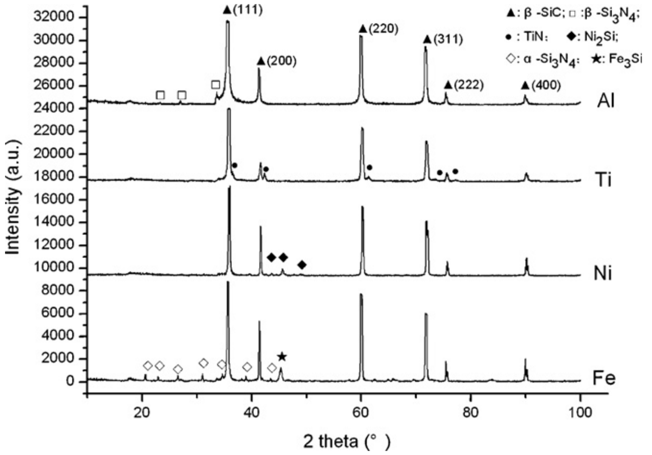

Fig. 2. XRD patterns of the products obtained from the samples with different metal catalysts in nitrogen atmosphere.

$\alpha$-$Si_3N_4$ peaks), upper parts of β-SiC (1 1 1), (2 2 0) and (3 1 1) peaks have been cut.

When Al powders were used as the catalyst, pale green free-flowing powders were obtained. The FESEM images (as shown Fig. 1(a)) show that the product consists mainly of particles with few nanowires. The XRD patterns (as shown in Fig. 2) demonstrate that the product is mainly β-SiC with traces of β-$Si_3N_4$. Mitomo [25] has reported that the addition of Al powders can promoted the growth of β-$Si_3N_4$. The peaks indicative of aluminum compounds cannot be found in the XRD patterns. Over the upper surface of the product we found a thin layer of white materials which contained lots of leaf-like and island-like crystals (Fig. 1(b)). The EDS (inset of Fig. 1(b)) shows that such crystals contain large amount of element Al, which indicates that quite a lot of Al was vaporized during the combustion process due to its low melting point (660 °C). This is the main reason why such few nanowires were grown when Al was used as the catalyst.

When Ti powders were used as the catalyst, the as-synthesized product has similar appearance to Al-catalyzed product. The FESEM images (shown in Fig. 1(c)) and XRD patterns (shown in Fig. 2) demonstrate that the product contains mainly β-SiC particles with small amount of TiN particles. The reason why no nanowires were grown with Ti catalyst is easily understood. During the combustion process, Ti powders rapidly reacted with $N_2$, producing solid-state TiN particles, and Ti/Si liquid which should be a key factor for the growth of nanowires was not produced. Therefore, Ti powders cannot catalyze the growth of nanowires in $N_2$ atmosphere.

When Ni or Fe powders were used as the catalyst, the as-obtained products were both found to be viscous powders. As shown in Fig. 1(d), the product obtained from Ni-catalyzed process is composed of particles and nanowires. These thin nanowires are randomly distributed among the particles. It can be clearly seen from the XRD pattern (Fig. 2) that the main phase of the product is β-SiC and the Ni catalyst worked in the form of $Ni_2Si$. The combustion temperature profile for the process with Fe catalyst (Fig. 5, 2 MPa $N_2$) shows that the temperature reached as high as 1337 °C during the CS. We suppose catalyst types have little influence on the combustion temperature. According to Ni–Si phase diagram, $Ni_2Si$ was completely in the liquid state at 1337 °C. Hence, Ni catalyst worked in the form of liquid Ni/Si alloy during the combustion process. Further characterization of the nanowires was carried out using TEM. As shown in Fig. 3(a), the nanowires have smooth surface and uniform diameters of 15–230 nm. The crystalline structures of the nanowires were examined using HRTEM and SAED. Fig. 3(b) depicts a typical HRTEM image with the corresponding SAED pattern of the nanowires, which demonstrate that the nanowires are $\alpha$-$Si_3N_4$ single crystals grown along the [1 0 1] direction. The HRTEM image reveals that the nanowires possess a perfect crystal structure with few structure defects.

As reported in our previous work [32], composite powders containing β-SiC particles and $\alpha$-$Si_3N_4$ nanowires (shown in

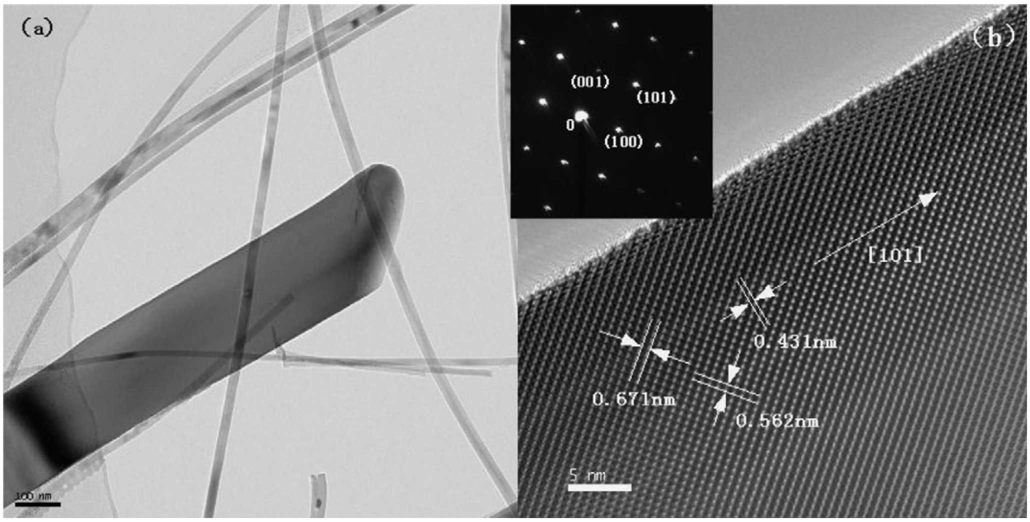

Fig. 3. (a) TEM image of the Ni-catalyzed nanowires. (b) HRTEM image with corresponding SAED pattern (inset) of one nanowire shown in (a). The measured *d* spacings of 0.671, 0.562 and 0.431 nm are in good agreement with (1 0 0), (0 0 1) and (1 0 1) planes of bulk $\alpha$-$Si_3N_4$ ($a$ = 7.758 Å, $c$ = 5.623 Å, PDF Card. No. 09-0250).

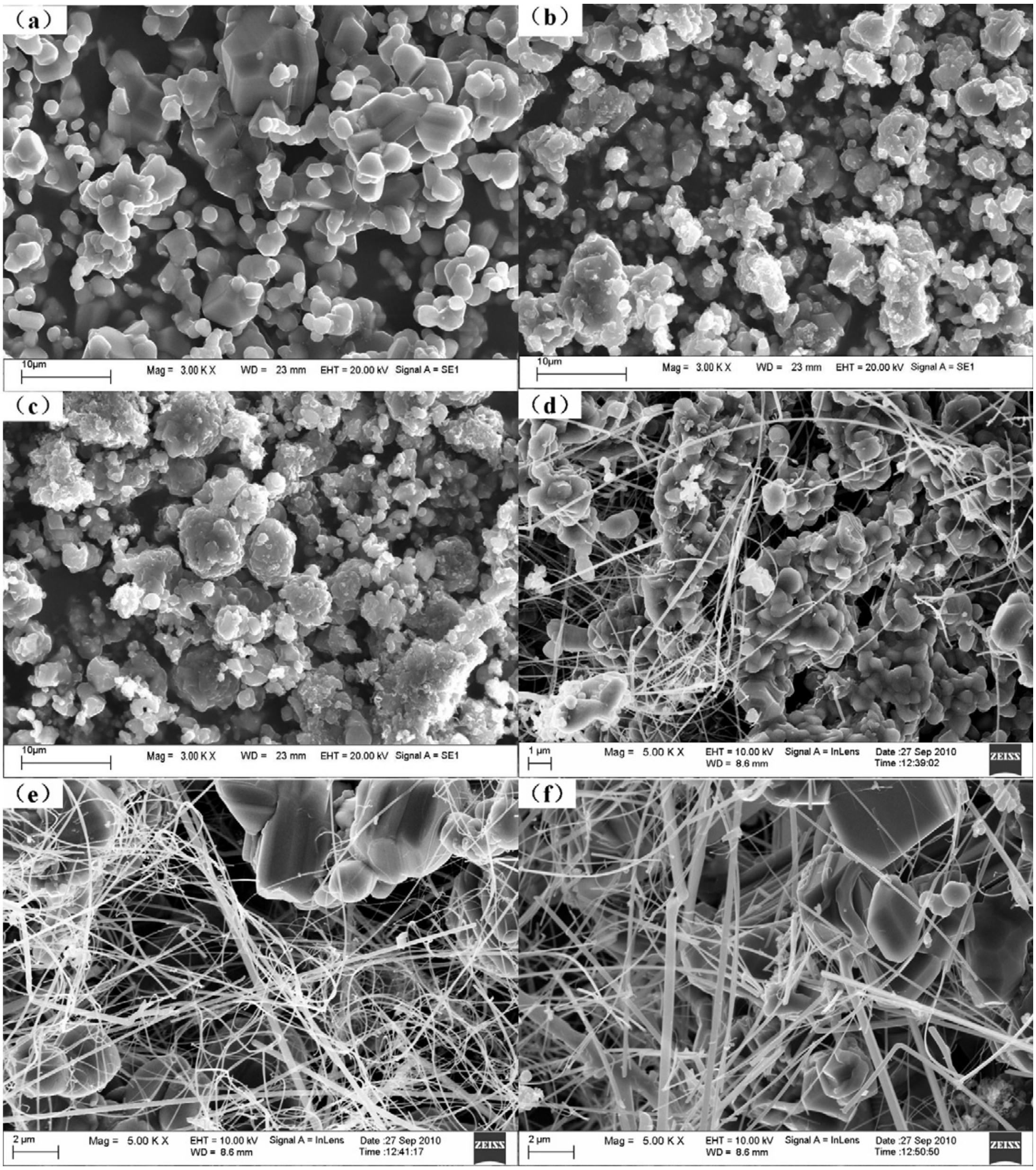

Fig. 4. FESEM images of the products synthesized under different conditions: (a) 2 MPa Ar; (b) 2 MPa $CO_2$; (c) 1.9 MPa $CO_2$ and 0.1 MPa $O_2$; (d) 0.6 MPa $N_2$; (e) 2 MPa $N_2$; (f) 4 MPa $N_2$.

Fig. 1(e)) could be obtained when Fe powders were used as the catalyst. The Fe catalyst worked in the form of $Fe_3Si$ (shown in Fig. 2) which is a key factor for the growth of nanowires. As shown in Fig. 1(d) and (e), Fe-catalyzed nanowires generally have larger diameters than Ni-catalyzed nanowires. We believe that the difference in diameters between Fe-catalyzed and Ni-catalyzed nanowires is ascribed to that the sizes of catalyst liquid are different. From Fe–C and Ni–C phase diagrams we can get that C has much higher solubility in Fe than that in Ni at about 1300 °C. When Fe and Ni powders have close diameters, Fe/Si alloy could absorb more carbon and formed a larger droplet than Ni/Si alloy during the combustion process, and larger droplets would produce larger $Si_3N_4$-NWs. So Fe-catalyzed nanowires have larger diameters than Ni-catalyzed ones. In this study, large $Si_3N_4$-NWs have more advantages to reinforce ceramics than small ones, and thus Fe powders are employed as the catalyst in later studies, which emphasize the influence of gas types and pressures. Besides, the combustion experiments were also carried out on the samples without the addition of metal catalyst and pure SiC particles were obtained.

It has been well known that transition metals can regulate the kinetics of silicon nitridation [25–31]. Here, if metal/silicon liquid (e.g. $Ni_2Si$ and $Fe_3Si$) could be formed during the combustion process, $Si_3N_4$-NWs were produced in addition to SiC particles. If not, only SiC particles were obtained (e.g. addition of Ti powders). Fig. 1(f) shows that, during the combustion process, the nanowires grew from the molten alloy

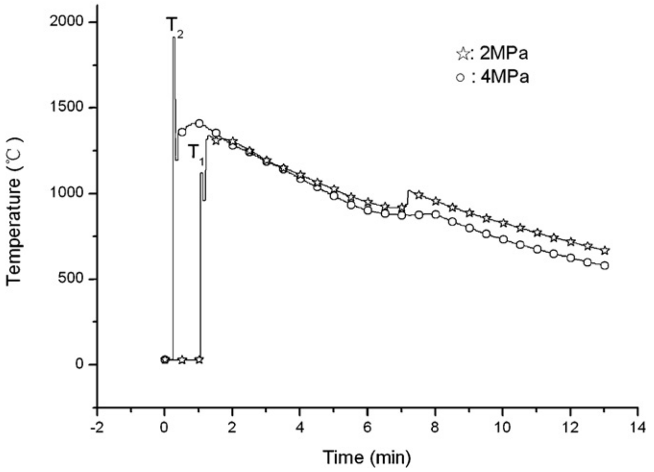

Fig. 5. Combustion temperature profiles for the processes under different nitrogen pressures.

by the SLGS mechanism, which has been carefully demonstrated in our previous work [32].

### 3.2. The gases

In addition to $N_2$, Ar, $CO_2$ and mixed $CO_2/O_2$ gases were employed as the combustion environments. For each process, Fe powders were used as the catalyst. The products obtained from Ar, $CO_2$ or mixed $CO_2/O_2$ gas are all green free-flowing powders. As shown in Fig. 4(a)–(c), the products synthesized in non-nitrogen gases are pure particles. XRD patterns reveal that the silicon has been completely transformed to β-SiC. This shows that the reaction between Si and PTFE can provide enough heat to activate the weak exothermic reaction between Si and C. Besides, the particles synthesized in Ar atmosphere possess more smooth surface than in $CO_2$ or mixed $CO_2/O_2$ atmosphere. This indicates that the SiC particles in Ar were mostly formed by the liquid-phase mechanism [4] while $CO_2$ and $O_2$ may have participated in the combustion reactions in $CO_2$ and mixed $CO_2/O_2$ atmosphere. As shown in Fig. 4(e), nanowires can be efficiently formed in $N_2$ atmosphere. Hence, we can get a conclusion that SiC whiskers cannot be formed under present conditions, which further confirms that the nanowires synthesized in $N_2$ atmosphere are $Si_3N_4$-NWs.

The combustion experiments were also carried out under different nitrogen pressures, using Fe as the catalyst. With rising initial pressure, the fibrous character of the products was enhanced, and as shown in Fig. 4(d)–(f), the nanowire content increased with nitrogen pressure. The enhancement of nanowire growth was especially distinct when the initial pressure was increased from 0.6 to 2 MPa. In addition, two kinds of SiC particles, namely small particles (below 1 μm, as shown in Fig. 4(d)) and large particles (1–10 μm, as shown in Fig. 4(f)), were observed within the products. The ratio of large particles in the products also increased with initial pressure. For the product synthesized under 4 MPa $N_2$, most of SiC particles belong to large particles. Fig. 5 depicts the combustion temperature profiles for the processes under 2 and 4 MPa nitrogen pressure. The combustion temperatures increased abruptly to $T_1$ (1120 °C) and $T_2$ (1912 °C) for 2 and 4 MPa nitrogen pressure respectively, which were ascribed to the highly exothermic nitridation of silicon [3], and dropped suddenly after several seconds. Subsequently, the temperatures increased again due to the other highly exothermic reaction between Si and PTFE. As shown in Fig. 5, the rise in nitrogen pressure results in significant increase in nitridation temperature, while they have similar temperature profiles during their later combustion periods. Hence, large amount of silicon liquid and metal/silicon liquid, which promoted the growth of large SiC particles and $Si_3N_4$-NWs respectively, could be rapidly formed under high nitrogen pressure. Besides, the nitrogen pressure can also influence the kinetics of reaction between silicon and nitrogen, and thus influence the yield of $Si_3N_4$-NWs.

### 3.3. The formation mechanisms

There are two main mechanisms, namely the gas-phase mechanism [3,5] and the liquid-phase mechanism [4,5], which have been proposed to explain the growth of SiC particles during the CS. For the CS carried out in $N_2$ in the present study, both of the two mechanisms were involved. During the process, silicon was firstly nitridated from the surface of each particle. This highly exothermic reaction produced large amount of heat, and the temperature increased rapidly. Then the initially formed $Si_3N_4$ decomposed by its own reaction heat and the released silicon vapor reacted with C to form SiC particles. The growth of SiC particles was dynamically favored because the vapor pressure of Si for $Si_3N_4$ is much higher than that for SiC [3]. The growth of small SiC particles (below 1 μm) was involved in this mechanism. As the combustion reactions proceeded, part of silicon particles were melted and C was dissolved in the molten silicon. Then large SiC particles (1–10 μm) were precipitated from the Si/C liquid. The growth of SiC was favored in the silicon liquid because the solubility of carbon in liquid silicon (e.g. 79 ppm at 1685 K) is higher than that of nitrogen (e.g. 4 ppm at 1685 K under 0.08 MPa) [33,34]. Hence, with rising $N_2$ pressure, more silicon particles were melted due to higher nitridation temperature and thus the ratio of large SiC particles was increased.

Our previous work [32] suggested that the growth mechanism of $Si_3N_4$-NWs synthesized via catalyst-assisted CS is a SLGS process. In this process, metal (M, e.g. Fe or Ni) powders initially reacted with Si and C particles to form Si–M–C alloy at a temperature higher than the eutectic temperature of Si–M–C ternary system. When the liquid alloy became supersaturated with Si and C, Si atoms within liquid alloy reacted with $N_2$ in the liquid/gas interface, and then $Si_3N_4$-NWs were precipitated from the liquid alloy due to its size confining effect (as shown in Fig. 1(f)). The kinetics of reaction between Si and $N_2$ was greatly promoted due to the presence of transition metal, which promote the growth of $Si_3N_4$-NWs. The liquid alloy was generally formed at the stage after nitridation when the temperature was relatively low, so α-$Si_3N_4$ crystals could be formed and $Si_3N_4$-NWs could be preserved instead of decomposition. Lastly, the carbon element within the alloy was precipitated with the temperature dropping.

## 4. Conclusions

In summary, we have completed a parametric investigation of fabrication of composite powders containing SiC particles and $Si_3N_4$-NWs by the CS. Elemental Si, carbon black, PTFE and small amount of metal powders were employed as raw materials. When metal/silicon liquid (e.g. $Ni_2Si$ and $Fe_3Si$) was formed during the combustion process in nitrogen, $Si_3N_4$-NWs were uniformly grown among the SiC particle. Contrarily, if no metal/silicon liquid was formed during the process in nitrogen (no catalyst or Ti as the catalyst) or the process was carried out in non-nitrogen gas (Ar, $CO_2$ or mixed $CO_2/O_2$), pure SiC particles were synthesized. The increase in nitrogen pressure can greatly promote the growth of $Si_3N_4$-NWs as well as large SiC particles. We conclude that the $Si_3N_4$-NWs were grown from the metal/silicon liquid by the SLGS mechanism, and the growth of SiC particles was involved in the gas-phase and liquid-phase mechanisms.

## Acknowledgment

This work was supported by Chinese National Fusion Project for ITER, under Grant No. 2010GB109000.

## References

[1] J.J. Moore, H.J. Feng, Combustion synthesis of advanced materials: Part I. Reaction parameters, Prog. Mater. Sci. 39 (4–5) (1995) 243–273.

[2] J.P. Lebrat, A. Varma, Combustion synthesis of the $YBa_2Cu_3O_{7-x}$ superconductor, Physica C 184 (4–6) (1991) 220–228.

[3] O. Yamada, K. Hirao, M. Koizumi, Y. Miyamoto, Combustion synthesis of silicon carbide in nitrogen atmosphere, J. Am. Ceram. Soc. 72 (9) (1989) 1735–1738.

[4] J. Narayan, R. Raghunathan, R. Chowdhury, K. Jagannadham, Mechanism of combustion synthesis of silicon carbide, J. Appl. Phys. 75 (11) (1994) 7252–7257.

[5] G. Liu, K. Yang, J. Li, K. Yang, J. Du, X. Hou, Combustion synthesis of nanosized $\beta$-SiC powder on a large scale, J. Phys. Chem. C 112 (16) (2008) 6285–6292.

[6] K. Yang, Y. Yang, Z.M. Lin, J.T. Li, J.S. Du, Mechanical-activation-assisted combustion synthesis of SiC powders with polytetrafluoroethylene as promoter, Mater. Res. Bull. 42 (9) (2007) 1625–1632.

[7] Y. Yang, Y.X. Chen, Z.M. Lin, J.T. Li, Synthesis of $\alpha$-$Si_3N_4$ using low-$\alpha$-phase $Si_3N_4$ diluent by the seeding technique, Scripta Mater. 56 (5) (2007) 401–404.

[8] Y. Chen, Z. Lin, J. Li, J. Du, S. Yang, PTFE, an effective additive on the combustion synthesis of silicon nitride, J. Eur. Ceram. Soc. 28 (1) (2008) 289–293.

[9] H.B. Jin, M.S. Cao, Y.X. Chen, J.T. Li, S. Agathopoulos, The influence of mechanochemical activation on combustion synthesis of $Si_3N_4$, Ceram. Int. 34 (5) (2008) 1267–1271.

[10] C.C. Agrafiotis, J. Lis, J.A. Puszynski, V. Hlavacek, Combustion synthesis of silicon nitride–silicon carbide composites, J. Am. Ceram. Soc. 73 (11) (1990) 3514–3517.

[11] J. Zeng, Y. Miyamoto, O. Yamada, Combustion synthesis of $Si_3N_4$–SiC composite powders, J. Am. Ceram. Soc. 74 (9) (1991) 2197–2200.

[12] D. Kata, J. Lis, R. Pampuch, Combustion synthesis of multiphase powders in the Si–C–N system, Solid State Ionics 101–103 (part 1) (1997) 65–70.

[13] A. Huczko, M. Bystrzejewski, H. Lange, A. Fabianowska, S. Cudziło, A. Panas, M. Szala, Combustion synthesis as a novel method for production of 1-D SiC nanostructures, J. Phys. Chem. B 109 (34) (2005) 16244–16251.

[14] A. Huczko, M. Osica, A. Rutkowska, M. Bystrzejewski, H. Lange, S. Cudziło, A self-assembly SHS approach to form silicon carbide nanofibres, J. Phys.: Condens. Matter 19 (2007) 395022.

[15] H. Chen, Y.G. Cao, J.X. Tang, S.Y. Tang, X. Chen, Fabrication of large-scale SiC fibers using carbamide as additives, J. Cryst. Growth 231 (1–2) (2001) 4–7.

[16] M.A. Rodriguez, N.S. Makhonin, J.A. Escriña, I.P. Borovinskaya, M.I. Osendi, M.F. Barba, et al., Single crystal $\beta$-$Si_3N_4$ fibers obtained by self-propagating high temperature synthesis, Adv. Mater. 7 (8) (1995) 745–747.

[17] Y.G. Cao, H. Chen, J.T. Li, C.C. Ge, S.Y. Tang, J.X. Tang, et al., Formation of $\alpha$-$Si_3N_4$ whiskers with addition of $NaN_3$ as catalyst, J. Cryst. Growth 234 (1) (2002) 9–11.

[18] J.V. Milewski, F.D. Gac, J.J. Petrovic, S.R. Skaggs, Growth of beta-silicon carbide whiskers by the VLS process, J. Mater. Sci. 20 (4) (1985) 1160–1166.

[19] S. Otoishi, Y. Tange, Growth rate and morphology of silicon carbide whiskers from polycarbosilane, J. Cryst. Growth 200 (3–4) (1999) 467–471.

[20] S.G. Sundaresan, A.V. Davydov, M.D. Vaudin, I. Levin, J.E. Maslar, Y.L. Tian, et al., Growth of silicon carbide nanowires by a microwave heating-assisted physical vapor transport process using group VIII metal catalysts, Chem. Mater. 19 (23) (2007) 5531–5537.

[21] G. Li, X. Li, Z. Chen, J. Wang, H. Wang, R. Che, Large areas of centimeters-long SiC nanowires synthesized by pyrolysis of a polymer precursor by a CVD route, J. Phys. Chem. C 113 (41) (2009) 17655–17660.

[22] P.C. Silva, J.L. Figueiredo, Production of SiC and $Si_3N_4$ whiskers in C + $SiO_2$ solid mixtures, Mater. Chem. Phys. 72 (3) (2001) 326–331.

[23] W. Yang, Z. Xie, J. Li, H. Miao, L. Zhang, L. An, Ultra-long single-crystalline $\alpha$-$Si_3N_4$ nanowires: derived from a polymeric precursor, J. Am. Ceram. Soc. 88 (6) (2005) 1647–1650.

[24] F. Wang, G.Q. Jin, X.Y. Guo, Formation mechanism of $Si_3N_4$ nanowires via carbothermal reduction of carbonaceous silica xerogels, J. Phys. Chem. B 110 (30) (2006) 14546–14549.

[25] M. Mitomo, Effect of Fe and Al additions on nitridation of silicon, J. Mater. Sci. 12 (2) (1977) 273–276.

[26] D.R. Messier, P. Wong, Kinetics of nitridation of Si powder compacts, J. Am. Ceram. Soc. 56 (9) (1973) 480–485.

[27] S.M. Boyer, A.J. Moulson, A mechanism for the nitridation of Fe-contaminated silicon, J. Mater. Sci. 13 (8) (1978) 1637–1646.

[28] H.M. Jennings, Review on reactions between silicon and nitrogen, Part 1: Mechanisms, J. Mater. Sci. 18 (4) (1983) 951–967.

[29] J. Mukerji, S.K. Biswas, Effect of iron, titanium, and hafnium on second-stage nitriding of silicon, J. Am. Ceram. Soc. 64 (9) (1981) 549–552.

[30] C.G. Cofer, J.A. Lewis, Chromium catalysed silicon nitridation, J. Mater. Sci. 29 (22) (1994) 5880–5886.

[31] V. Pavarajarn, S. Kimura, Catalytic effects of metals on direct nitridation of silicon, J. Am. Ceram. Soc. 84 (8) (2001) 1669–1674.

[32] C.S. Zheng, Q.Z. Yan, M. Xia, C.C. Ge, In situ preparation of SiC/$Si_3N_4$-NW composite powders by combustion synthesis, Ceram. Int. (2011), doi:10.1016/j.ceramint.2011.07.032.

[33] K. Yanaba, M. Akasaka, M. Takeuchi, M. Watanabe, T. Narushima, Y. Iguchi, Solubility of carbon in liquid silicon equilibrated with silicon carbide, Mater. Trans., JIM 38 (11) (1997) 990–994.

[34] T. Narushima, N. Ueda, M. Takeuchi, F. Ishii, Y. Iguchi, Nitrogen solubility in liquid silicon, Mater. Trans., JIM 35 (11) (1994) 821–826.